

Numerical Stability of Plane Crack Paths under Mode I Loading Conditions

Rayk Thumser

rayk.thumser@mfpa.de, MFPA Weimar, Coudraystraße 9, 99423 Weimar, Germany

ABSTRACT. *Advanced life predictions in cyclically loaded components consider both crack initiation and crack propagation phase with its quite different damage mechanisms. In components under internal cyclic pressure loading the notches are located in the pressurized inside, so that crack initiation and crack propagation cannot be observed directly. Usually only the total life up to the leakage of the component can be determined. Due to the lack of experimental data for crack initiation and crack growth phases the corresponding life predictions cannot be validated separately. A method for automatic crack growth calculation with FE is presented. For the numerical crack growth simulation the crack increment size influences directly the crack shape development. Too large increments cause numerical instability. To reach the numerical stability model extensions are presented and explained. The comparisons of the calculated cycles to experimental results show a good agreement.*

INTRODUCTION

Pressures in cyclically loaded components are continuously rising, e.g. in Diesel injection parts. To meet these challenges life prediction methods were developed and verified by experiments with some hundred notched specimens [1–4]. There are only experimental final fracture data available. The prediction methods always combine crack initiation and crack growth. The sum of crack initiation and crack growth lives can then be compared to the experimental final fracture lives.

Today's requirements for fatigue strength can only be achieved by autofrettage or case hardening. In the autofrettage process a single internal pressure overload generates a compressive residual stress field in the notch leading to an increase of fatigue strength up to a factor of 3.5 [1]. The case hardening process also increases the fatigue strength considerably [2] and additionally improves the wear and cavitation pitting resistance.

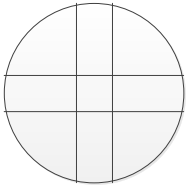
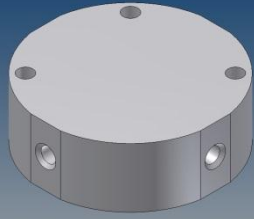
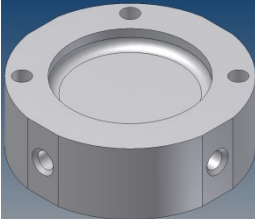
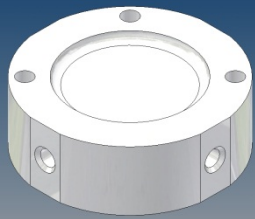
INVESTIGATION PROGRAM

Cross bore specimens

A typical feature of an internal pressure loaded component is the intersection of two borings. For research purposes cross bore specimens were developed, as shown in table 1. This design is multi symmetric. The cross bore specimens are disks with

perpendicular borings of 5 mm with different disk middle thicknesses. The thicknesses were designed in a way that the fatigue strengths of all three specimens are about 2000 bar. More details can be found at [5], [6].

Table 1 Cross bore specimens

			
Material	42CrMo4 (DIN 1.7725) quenched and tempered		18CrNiMo7-6 (DIN 1.6587) case hardened
Disk diameter	58 mm		
Bore diameter d	5 mm		
Disk middle height h	20 mm	10 mm	15 mm
h / d	20 / 5	10 / 5	15 / 5
Autofrettage	-	6000 bar	-

Load sequences

There are two tested load sequences, pure dwell with about $R=0$ and a two level test with the small cycles at the maximal pressure, figures 1 and 2.

SIMULATION OF CRACK GROWTH WITH LEBM

Crack Growth Model

The crack growth model is based on the LEFM. The stress intensity factors (SIF) are evaluated for different load cases:

- unit pressure on the boring
- unit pressure on the crack face
- residual stresses from the uncracked model as crack face loading for the crack model using the superposition principle

The autofrettage residual stress calculation is the addition of load and unload stresses from autofrettage load and unload [4], [7], [8]. Using the Rainflow algorithm [9], [10] for the load sequences the minimum and maximum SIF can be evaluated on the superposition of scaled SIF from pressure on bores and the crack face and the SIF from residual stresses. The formulas from Ibrahim et. al. [11] are successfully applied to crack growth simulation with the weight function method [4] to estimate the crack opening behaviour, eq. 1.

$$\frac{S_{op}}{S_{max}} = \alpha \left[1 - \beta \left(\frac{S_{max}}{\sigma_y} \right)^\gamma \right] \quad (1)$$

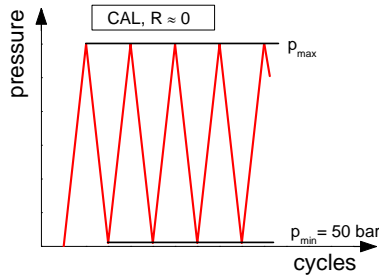


Figure 1 Constant amplitude loading (CAL) R=0

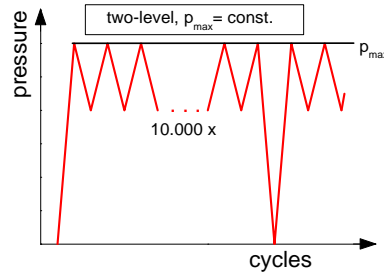


Figure 2 Two-level load sequence

To estimate the nominal stresses S the SIF where transferred into a constant stress distribution which results in the same SIF. This means that for pressure on the crack face the stresses S is equivalent to the pressure loading. This leads to an equivalent SIF range ΔK_{eff} .

The crack growth relationship here used is a Paris-Erdogan [12] law for equivalent SIF ranges:

$$\frac{da}{dN} = C_0 \left[\frac{\Delta K_{eff}}{\Delta K_{eff,0}} \right]^m \quad (2)$$

Crack Growth Simulation Program

The crack growth procedure is realised as Python script for Abaqus 6.10 [13]. The Python Language [14] allows a fully automatic execution of pre- and post-processing as well as execution of FE-solver. The SIF for the different load cases where calculated using the built in function of Abaqus.

The cross bore specimen where modelled by 1/16 using all symmetries. The script generates the model with the crack in middle symmetric plane. After the execution of the FE-solver the crack increment is calculated for each crack front node and per cycle from the Rainflow algorithm. After a defined maximum increment a new loop cycle is created automatically.

Crack Growth Simulation Parameters

For the crack growth relationship Vormwald [15] parameter are used

$$\frac{da}{dN} = 10^{-5} \text{ mm} \left[\frac{\Delta K_{eff}}{9,0 \text{ MPa}\sqrt{\text{m}}} \right]^{3,0} \quad (3)$$

As threshold value for crack stop $\Delta K_{eff,th} = 3,5 \text{ MPa}\sqrt{\text{m}}$ is taken. An initial crack size of $0,25 \text{ mm}$ is used as initial crack. The calculation is stopped at a crack length of 10 mm .

To get smooth crack front the maximum clearance of the crack front nodes is limited. As well as the minimum clearance between two crack front nodes I limited to 60 percent of the allowable maximum clearance. So a smooth crack front mesh is secured. For the evaluation of SIF the FE-mesh has to be hexahedral around the crack. Figure 3 shows a FE-model with different zoom factors with a crack front and crack depth of 1.8 mm at the symmetric plane (45 degree).

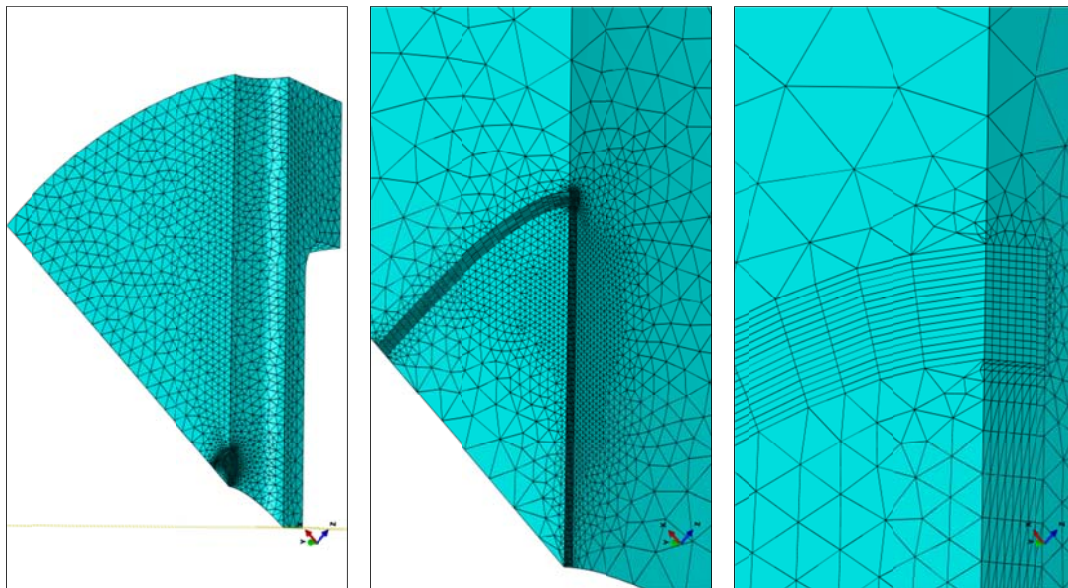


Figure 3 Script generated FE-model of with crack front

While the full recalculation of SIF is not done cycle per cycle there are some stabilization techniques are required. Fulland and Fulland and Richard [16–18] suggested a minimum crack increment. Kolk, Kolk and Kuhn and Weber and Kuhn introduce [19–21] an explicit predictor – corrector step. Thumser [22] suggested an averaging of the SIF and the crack increments.

In this investigation the SIF are averaged by weighted sliding mean value along the crack front:

$$K_i^{weighted} = \frac{1}{\sum_{j=-2}^{+2} [w_j]} \sum_{j=-2}^{+2} [w_j \cdot K_{i+j}]. \quad (4)$$

The corresponding weights $w_{i(-2...+2)}$ are 0.50, 0.75, 1.00, 0.75, 0.50. The averaging is needed to compensate numerical deviations in the FE-Solution, e.g. the SIF at middle nodes of quadratic elements are always different from corner node solutions. The Paris law with the exponent of 3.0 also increases the small deviations.

To get a script automatically run the crack increment has to be limited to geometric conditions. For these calculations the maximum allowable crack increment is the minimum of following:

- 5 percent of actual crack length and
- 90 percent of maximum clearance between crack front nodes.

Within these settings the calculation from 0.25 mm to 10 mm needs about 200 loops. The averaging time for one loop is about 15 minutes so the overall computational time is about 50 hours on an 2xXeon E645 @2.4GHz.

A quality control of the crack growth calculation parameters is the analysis of the effective SIF along the crack front. The crack itself tends to have the same crack growth speed along the crack front; this means the same effective SIF along the crack front. A deviation of a maximum of 8 percent from min to max effective SIF along the crack front was observed.

By increasing these maximum allowable crack increment the crack front becomes numerical instable. Then in some cases the crack front shape looks like a sawtooth.

COMPARISON TO EXPERIMENTAL RESULTS

The fatigue tests with internal pressure loading leads only to the sum of crack initiation life and crack growth life. Therefore the crack initiation life to 0.25 mm has to be calculated.

Simulation of Crack initiation

The crack initiation life has been calculated with the Local Approach [23]. Details can be found at [4], [5].

Comparison to experimental results

Here only the results are shown for the cross bore specimen in autofretted condition. For the other two specimens details can be found at [5]. The comparison for CAL shows a good agreement to the experimental results. The most important part is the crack growth life, fig. 4. For the two-level tests the ratio of crack initiation life and crack growth life depends on the load level. fig. 5. The results are in the same good agreement as for the CAL.

CRACK SHAPE DEVELOPMENT AND POSSIBLE SIMPLIFICATIONS

For the CAL and the two-level test the crack shape stays nearly quarter circular. The difference of SIF under 45 degrees are nearly the same. So the calculation could be simplified with an assumption of quarter circular crack. The SIF can be calculated within one FE-calculation using nodal release technique. With this the crack growth calculation becomes a post-processing step. With the results of these FE-calculation using nodal release technique all load sequences and load levels can be calculated.

One exception has to be made. The crack arrest shape for CAL does not stay quarter circular, figs. 6 and 7. The presented procedure can evaluate the crack arrest shape as well as the crack arrest pressure.

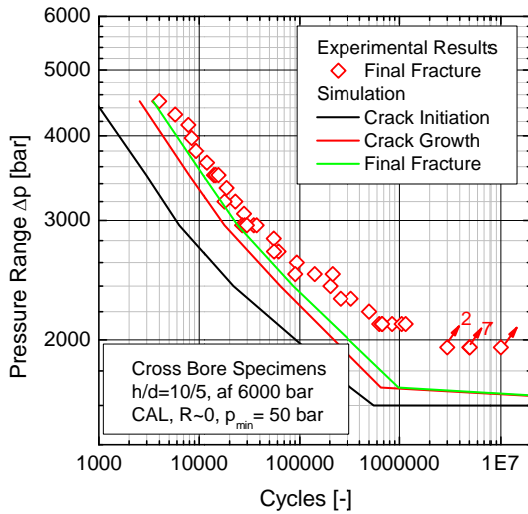


Figure 4 Predictions and experimental results for CAL

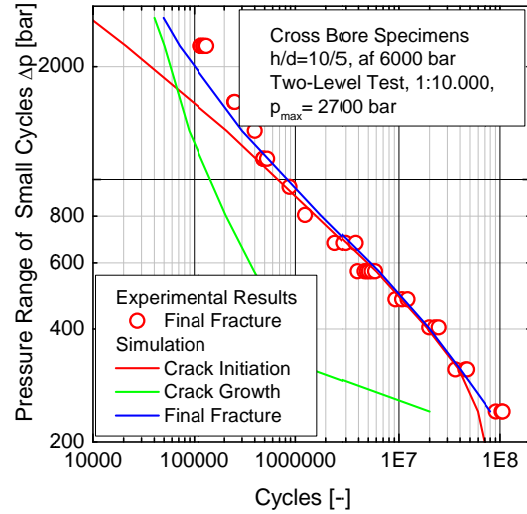


Figure 5 Predictions and experimental results for two-level tests

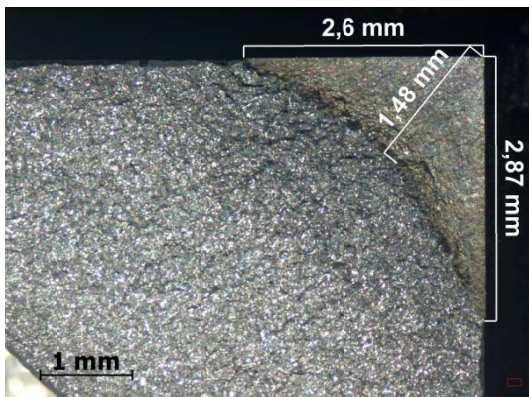


Figure 6 Fractographic determined crack arrest, from [22]

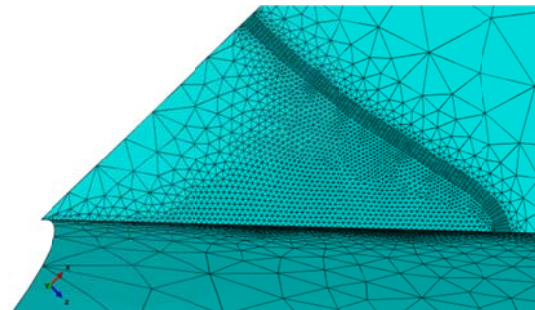


Figure 7 Crack arrest contour, crack length 1.0 mm and 1.6 mm

SUMMARY

The presented procedure show a good stability for automated crack growth calculation with free shape development for mode I loading. To reach the numerical stability model extensions are presented and explained. The comparisons of the calculated cycles to experimental results show a good agreement.

ACKNOWLEDGEMENTS

The authors thank the Federal Ministry of Economics and Technology, the German Federation of Industrial Research Associations ‘Otto von Guericke’ e.V. (AiF-Nr. 16023 B) and the ‘Forschungsvereinigung Verbrennungskraftmaschinen’ e.V. (FVV) for their financial support.

REFERENCES

- [1] T. Seeger, M. Schön, J. W. Bergmann, and M. Vormwald, “Autofrettage I: Vorhaben Nr. 478; Dauerfestigkeitssteigerung durch Autofrettage; Abschlußbericht; Forschungsberichte Verbrennungskraftmaschinen, Heft 550,” Forschungsvereinigung Verbrennungskraftmaschinen e. V. (FVV), Frankfurt, 1993.
- [2] A. Diemar, K. Linne, J. W. Bergmann, and M. Vormwald, *Einsatzhärten und Autofrettage; Vorhaben Nr. 784; Dauerfestigkeitssteigerung einsatzgehärteter Hochdruckbauteile durch Autofrettage; Abschlußbericht; Heft 783*. Frankfurt: Forschungsvereinigung Verbrennungskraftmaschinen e. V. (FVV), 2004.
- [3] T. Seeger, S. Greuling, and J. W. Bergmann, “Autofrettage II: Vorhaben Nr. 671; Dauerfestigkeitssteigerung durch Autofrettage II; Abschlußbericht; Heft 704,” Forschungsvereinigung Verbrennungskraftmaschinen e. V. (FVV), Frankfurt, 2001.
- [4] R. Thumser, E. Herz, O. Hertel, J. W. Bergmann, and M. Vormwald, *Betriebsfestigkeit Hochdruckbauteile: Vorhaben Nr. 880; Betriebsfestigkeit gekerbter Hochdruckbauteile ohne und mit Autofrettage; Abschlussbericht*. Frankfurt am Main: FVV, 2009.
- [5] R. Thumser, S. Kleemann, A. Diemar, U. Gerth, A. Kleemann, Y. Pan, T. Beier, M. Kaffenberger, A. Rosetti, T. Schlitzer, P. Zerres, J. W. Bergmann, and M. Vormwald, *Betriebsfestigkeit von Hochdruckbauteilen mit kleinen Schwingspielen großer Häufigkeit: Vorhaben Nr. 1000; Abschlussbericht*. Frankfurt am Main: FVV, 2012.
- [6] R. Thumser, M. Schickert, S. Kleemann, J. Winge, and U. Gerth, “Crack Growth Measurements in Notches Under Cyclic Internal Pressure Loading,” in *Proc. of Eighteenth European Conference on Fracture*, Dresden, 2010.
- [7] R. Thumser, J. W. Bergmann, and M. Vormwald, “Design of Autofretted Diesel Engine Injection Components Based on Fracture Mechanics,” in *Pressure Vessel and Piping - Design and Analysis*, ASME, 2001, pp. 203–208.
- [8] R. Thumser, J. W. Bergmann, and M. Vormwald, “Residual Stress Fields and Fatigue Analysis of Autofretted Parts,” *International Journal of Pressure Vessels and Piping*, vol. 79, no. 2, pp. 113–117, 2002.
- [9] U. H. Chlormann and T. Seeger, “Rainflow HCM - Ein Verfahren für Betriebsfestigkeitsnachweise auf werkstoffmechanischer Grundlage,” *Stahlbau*, vol. 55, no. 3, pp. 65–71, 1986.
- [10] M. Matsuiski and K. Endo, “Fatigue of Metals Subjected to Varying Stress,”

- Japan Soc. Mech. Engrg.*, 1969.
- [11] F. K. Ibrahim, J. C. Thompson, and T. H. Topper, "A study of the effect of mechanical variables on fatigue crack closure and propagation," *International Journal of Fatigue*, vol. 8, no. 3, pp. 135–142, 1986.
 - [12] P. C. Paris and F. Erdogan, "A Critical Analysis of Crack Propagation Laws," *Journal of Basic Engineering*, vol. 85, pp. 528–534, 1960.
 - [13] *ABAQUS 6.10 EF-1*. Dassault Systems, 2010.
 - [14] "Python Programming Language - Official Website." [Online]. Available: <http://python.org/>. [Accessed: 11-Jan-2012].
 - [15] M. Vormwald, "Anrisslebensdauervorhersage auf der Basis der Schwingbruchmechanik für kurze Risse," TH Darmstadt, Institut für Stahlbau und Werkstoffmechanik, 1989.
 - [16] M. Fulland, "Rissimulationen in dreidimensionalen Strukturen mit automatischer adaptiver Finite-Elemente-Netzgenerierung," Universität Paderborn, Fachgruppe Angewandte Mechanik (FAM), 2003.
 - [17] M. Fulland and H. A. Richard, "Finite-Element-Based Fatigue Crack Growth Simulation in Real Structures," *Key Engineering Materials*, vol. 251–252, pp. 79–84, 2003.
 - [18] M. Schöllmann, M. Fulland, and H. . Richard, "Development of a New Software for Adaptive Crack Growth Simulations in 3D Structures," *Engineering Fracture Mechanics*, vol. 70, no. 2, pp. 249–268, Jan. 2003.
 - [19] K. Kolk, *Automatische 3D-Rissfortschrittssimulation unter Berücksichtigung von 3D-Effekten und Anwendung schneller Randelementformulierungen*. Düsseldorf: VDI-Verl., 2005.
 - [20] K. Kolk and G. Kuhn, "A Predictor-Corrector Scheme for the Optimization of 3D Crack Front Shapes," *Fatigue & Fracture of Engineering Materials and Structures*, vol. 28, pp. 117–126, Jan. 2005.
 - [21] W. Weber and G. Kuhn, "An Optimized Predictor - Corrector Scheme for Fast 3D Crack Growth Simulations," *Engineering Fracture Mechanics*, vol. 75, no. 3–4, pp. 452–460, Feb. 2008.
 - [22] R. Thumser, "Simulation des Rissfortschritts in autofrettierten und nicht autofrettierten Bohrungsverschneidungen auf der Grundlage der linear-elastischen Bruchmechanik," Dissertation, Bauhaus Universität Weimar, Fakultät Bauingenieurwesen, 2009.
 - [23] J. W. Bergmann, "Zur Betriebsfestigkeit gekerbter Bauteile auf der Grundlage der örtlichen Beanspruchungen," Dissertation, TU Darmstadt, Institut für Stahlbau und Werkstoffmechanik, 1983.